A phosphorylated zinc finger peptide bearing a Gadolinium complex for zinc detection by MRI

Kyangwi P. Malikidogo,[a] Agnès Pallier,[b] Frédéric Szeremeta, [b] Célia S. Bonnet [*b] and Olivier Sénèque [*a]

[a] Univ. Grenoble Alpes, CNRS, CEA, IRIG, LCBM (UMR 5249), F-38000 Grenoble

[b] Centre de Biophysique Moléculaire, CNRS (UPR 4301), Université d'Orléans, F-45041 Orléans, France.

Electronic Supporting Information

Content

Abbreviations

Boc: *tert*-butyloxycarbonyl; **CD:** circular dichroism; **DCM:** dicholoromethane; **DIEA:** *N*,*N*-diisopropylethylamine; **DMF:** *N*,*N*-dimethylformamide; **ESI:** electrospray ionization; **Et_2O:** diethylether; **Fmoc:** 9-fluorenylmethoxycarbonyl; **HCTU:** 2-(6-chloro-1-H-benzotriazole-1-yl)-1,1,3,3-tetramethylaminium hexafluoro-phosphate; **HEPES:** hydroxyethyl-piperazineethane-sulfonic acid; **HPLC:** high performance liquid chromatography; **MeCN:** acetonitrile; **LRMS:** low resolution mass spectrometry; **NMRD:** Nuclear Magnetic Relaxation Dispersion; **$Pd(PPh_3)_4$:** *tetrakis*(triphenylphosphine)-palladium(0); **PyBOP:** (benzotriazol-1-yloxy)tripyrrolidino-phosphonium hexafluorophosphate; **SBM:** Solomon-Bloembergen-Morgan; **tBu:** *tert*-butyl; **TCEP:** *tris*(2-carboxyethyl)phosphine ; **TFA:** trifluoroacetic acid; **Trt:** trityl ; **UV-Vis:** ultraviolet-visible

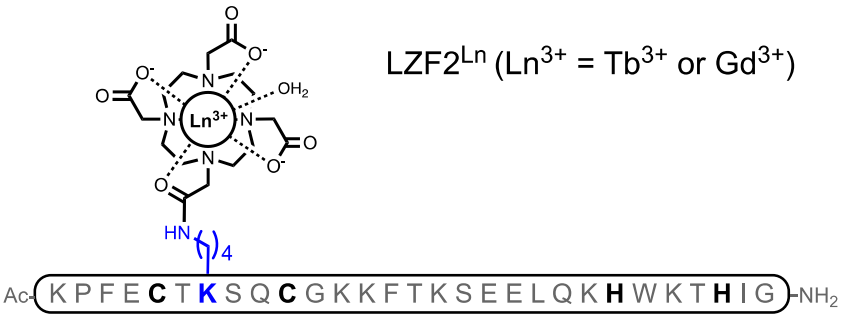

Fig. S1: Sequence of $LZF2^{Ln}$ (Ln = Tb or Gd).

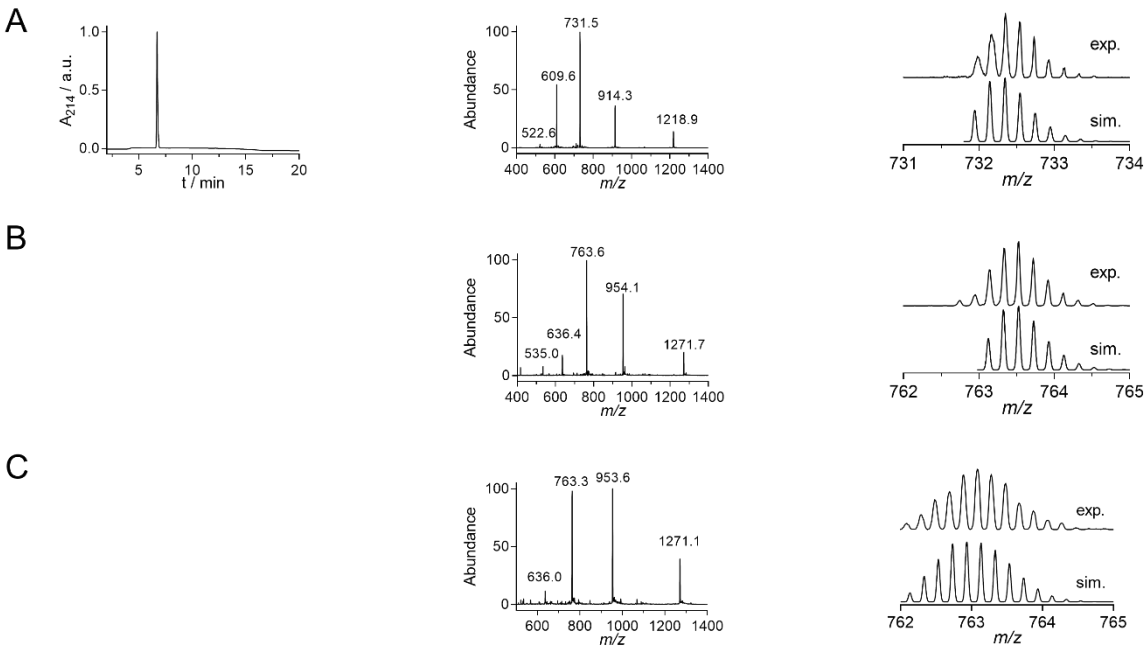

Fig. S2: HPLC chromatogram and ESI-MS spectra of ZFQE (A), ESI-MS spectra of ZFQE^{Tb} (B) and ZFQE^{Gd} (C).

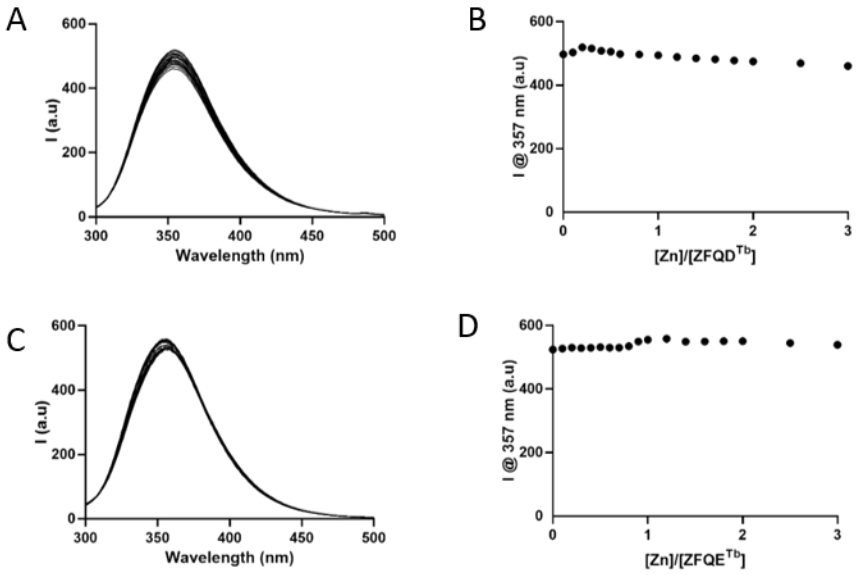

Fig. S3: A and B) Evolution of the tryptophan fluorescence emission (λ_{ex} = 280 nm) upon addition of Zn^{2+} in a solution of ZFQD^{Tb} (100 µM). C and D) Evolution of the tryptophan fluorescence emission (λ_{ex} = 280 nm) upon Zn^{2+} addition in a solution of ZFQE^{Tb} (20 µM). Samples were prepared in unbuffered water, pH adjusted to 7.4 for CD and in a HEPES buffer (10 mM, pH 7.4) containing 250 µM TCEP for luminescence.

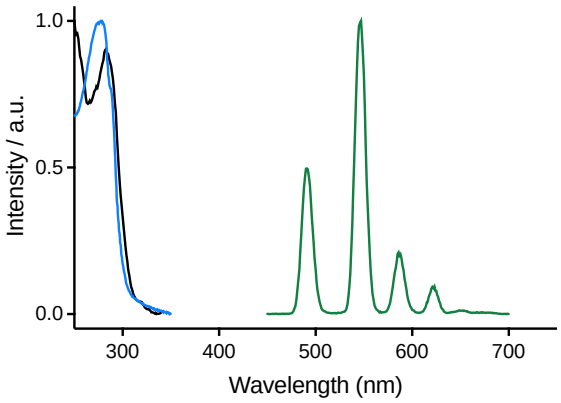

Fig. S4: Absorption (blue) and time-gated Tb^{3+} luminescence excitation (black, λ_{em} = 545 nm, delay = 0.1 ms) and emission (green, λ_{ex} = 280 nm, delay = 0.1 ms) spectra of $ZFQE^{Tb}$ in HEPES buffer (10 mM, pH 7.4).

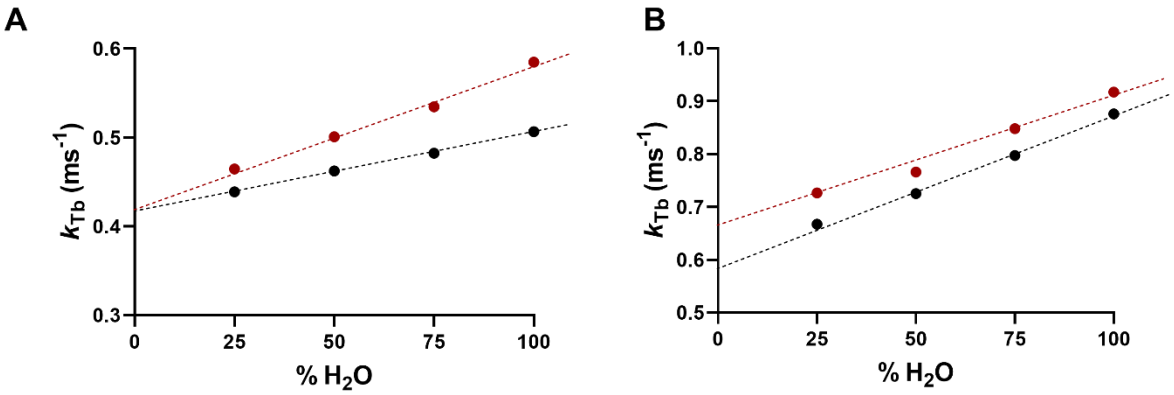

Fig. S5: Plot of the Tb^{3+} luminescence decay rate constants k_{Tb} against the volume fraction of H_2O in H_2O/D_2O mixtures for free (black) and Zn-loaded (red) $ZFQE^{Tb}$ (A) and $ZFQD^{Tb}$ (B).[1] Decays were recorded in a HEPES buffer (10 mM, pH 7.4) containing 250 µM TCEP.

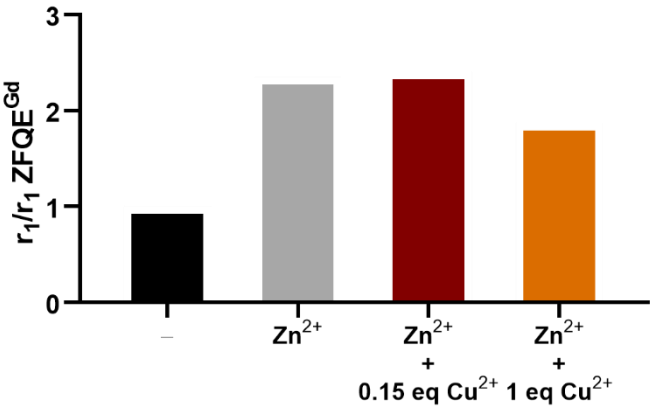

Fig. S6: Selectivity plot obtained by measuring the relaxivity of $ZFQE^{Gd}$ (0.38 mM) alone (left) or in the presence of 1 eq. of Zn^{2+}, to which 0.15 eq. or 1 eq. of Cu^{2+} have been added. All solutions were prepared in HEPES buffer solution (100 mM, pH 7.4, 25 mM TCEP).

Table S1. Best-fit parameters obtained from the fitting of the ^{1}H NMRD profiles to the SBM theory.

Parameters	$ZFQE^{Gd}$
q^a	1
k_{ex}^{298} (10^6 s^{-1})^a	111
$\Delta H^{\neq}$ (kJ mol^{-1})^a	21
E_R (kJ mol^{-1})	22 ± 4
τ_R^{298} (ps)	990 ± 50
E_V (kJ mol^{-1})^a	1
τ_V^{298} (ps)	13 ± 3
Δ^2 (10^{19} s^{-2})	0.09 ± 0.01

^{a} Fixed during the fitting procedure.

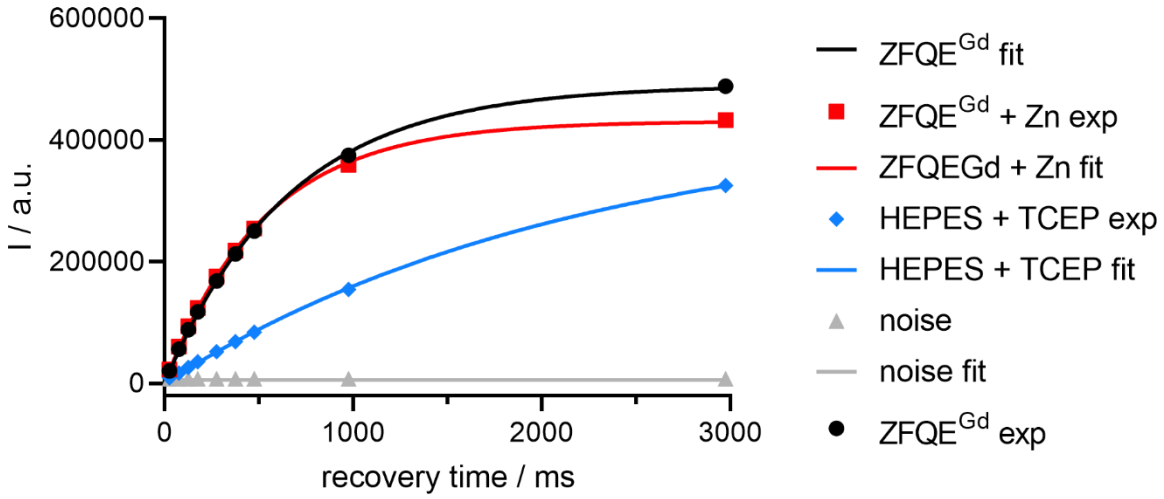

Fig. S7. Mean intensity of phantoms of ZFQE^{Gd} (●), Zn-ZFQE^{Gd} (■) and HEPES (◆), and of background noise (▲) measured on MRI images acquired at a fixed TE value of 9.9 ms, with 9 different TR values ranging from 25 ms to 3000 ms. Images were acquired with a spin echo sequence at 9.4 T, with a BioSpec 94/20 Bruker spectrometer. An exponential fitting of these curves allows measurement of the T1 relaxation time constants of the phantoms.

Equations used for the analysis of the NMRD data

The measured longitudinal proton relaxation rate, R_1^{obs} is the sum of the paramagnetic and diamagnetic contributions as expressed in Eq. 1, where r_1 is the proton relaxivity:

$$R_1^{obs} = R_1^d + R_1^p = R_1^d + r_1 \times c_{Gd} \quad [1]$$

The relaxivity can be divided into terms of inner and outer sphere, as follows:

$$r_1 = r_{1is} + r_{1os} \quad [2]$$

The inner sphere term is obtained in Eq. 3, where q is the number of inner sphere water molecules.[2]

$$r_{1is} = \frac{1}{1000} \times \frac{q}{55.55} \times \frac{1}{T_{1m}^H + \tau_m} \quad [3]$$

The longitudinal relaxation rate of inner sphere protons, $1/T_{1m}{}^H$ is expressed by Eq. 4, where r_{GdH} is the effective distance between the electron charge and the ^{1}H nucleus, ω_I is the proton resonance frequency and ω_S is the Larmor frequency of the Gd^{III} electron spin.

$$\frac{1}{T_{1m}^{H}} = \frac{2}{15}\left(\frac{\mu_0}{4\pi}\right)^2 \frac{\hbar^2 \gamma_I^2 \gamma_S^2}{r_{GdH}^6} S(S+1) \times \left[3J(\omega_I ; \tau_{d1}) + 7J(\omega_S ; \tau_{d2})\right] \quad [4]$$

$$\frac{1}{\tau_{di}} = \frac{1}{\tau_m} + \frac{1}{\tau} + \frac{1}{T_{ie}} \quad [5]$$

The longitudinal and transverse electronic relaxation rates, $1/T_{1e}$ and $1/T_{2e}$ are expressed by Eq. 6-7, where τ_V is the electronic correlation time for the modulation of the zero-field-splitting interaction, E_V the corresponding activation energy and Δ^2 is the mean square zero-field-splitting energy. We assumed a simple exponential dependence of τ_V versus $1/T$.

$$\left(\frac{1}{T_{1e}}\right)^{ZFS} = \frac{1}{25}\Delta^2 \tau_v \left\{4S(S+1) - 3\right\}\left(\frac{1}{1+\omega_S^2 \tau_v^2} + \frac{4}{1+4\omega_S^2 \tau_v^2}\right) \quad [6]$$

$$\left(\frac{1}{T_{2e}}\right)^{ZFS} = \Delta^2 \tau_v \left(\frac{5.26}{1+0.372\omega_S^2 \tau_v^2} + \frac{7.18}{1+1.24\omega_S \tau_v}\right) \quad [7]$$

$$\tau_v = \tau_v^{298} \, exp\left\{\frac{E_v}{R}\left(\frac{1}{T} - \frac{1}{298.15}\right)\right\} \quad [8]$$

The outer-sphere contribution can be described by Eq. 5 where NA is the Avogadro constant, and Jos is its associated spectral density function.[3,4]

$$r_{1os} = \frac{32 N_A \pi}{405}\left(\frac{\mu_0}{4\pi}\right)^2 \frac{\hbar^2 \gamma_S^2 \gamma_I^2}{a_{GdH} D_{GdH}} S(S+1)\left[3J_{os}(\omega_I, T_{1e}) + 7J_{os}(\omega_S, T_{2e})\right] \quad [9]$$

$$J_{os}(\omega, T_{je}) = Re\left[\frac{1 + \frac{1}{4}\left(i\omega\tau_{GdH} + \frac{\tau_{GdH}}{T_{je}}\right)^{1/2}}{1 + \left(i\omega\tau_{GdH} + \frac{\tau_{GdH}}{T_{je}}\right)^{1/2} + \frac{4}{9}\left(i\omega\tau_{GdH} + \frac{\tau_{GdH}}{T_{je}}\right) + \frac{1}{9}\left(i\omega\tau_{GdH} + \frac{\tau_{GdH}}{T_{je}}\right)^{3/2}}\right] \quad j = 1, 2 \quad [10]$$

The diffusion coefficient for the diffusion of a water proton away from a Gd^{III} complex, D_{GdH}, is assumed to obey an exponential law versus the inverse of the temperature, with an activation energy E_{GdH}, as given in Eq. 11 D_{GdH}^{298} is the diffusion coefficient at 298.15 K.

$$D_{\mathrm{GdH}} = D_{\mathrm{GdH}}^{298} \exp\left\{ \frac{E_{\mathrm{GdH}}}{R} \left(\frac{1}{298.15} - \frac{1}{T} \right) \right\} \qquad [11]$$

References

1 A. Beeby, I. M. Clarkson, R. S. Dickins, S. Faulkner, D. Parker, L. Royle, A. S. de Sousa, J. A. G. Williams and M. Woods, *J. Chem. Soc. Perkin Trans. 2*, 1999, 493–504.
2 Z. Luz and S. Meiboom, *J. Chem. Phys.*, 1964, **40**, 2686–2692.
3 J. H. Freed, *J. Chem. Phys.*, 1978, **68**, 4034–4037.
4 S. H. Koenig and R. D. Brown, *Prog. Nucl. Magn. Reson. Spectrosc.*, 1990, **22**, 487–567.